Program Digest, 2019 IEEE International Ultrasonics Symposium (IUS)
Glasgow, Scotland, October 6-9, 2019

Removal of Stress Hillocks from Platinum-Alumina Electrodes Used in High-temperature SAW Devices

Armando Ayes
Frontier Institute for Research in Sensor Technologies
Dept. of Electrical and Comp. Eng.
University of Maine
Orono ME, USA
armando.ayes@maine.edu

George Bernhardt
Frontier Institute for Research in Sensor Technologies
Dept. of Physics and Astronomy
University of Maine
Orono ME, USA
georgeb@maine.edu

Mauricio Pereira da Cunha
Frontier Institute for Research in Sensor Technologies
Dept. of Electrical and Comp. Eng.
University of Maine
Orono ME, USA
mdacunha@maine.edu

***Abstract*—Microwave acoustic devices operating at elevated temperatures, such as surface acoustic wave (SAW) duplexers or high-temperature sensors, require stable thin film electrodes capable of operating in such conditions. Stresses at the interface between the substrate and the thin film electrodes originated during electrode deposition and/or during device operation can foster film agglomeration, formation of whiskers, hillocks, electromigration, separation of the metal and oxide in composite electrodes, which degrade the electrode conductivity and the device's long-term stability and performance. Thin film composite Pt-Al_2O_3 has been successfully used as electrodes in langasite (LGS) SAW devices and sensors up to 900°C, but the formation of hillocks due to stress is seen as a limitation to the device long-term stability. In this work, a modified graded film deposition technique has been implemented targeting the release of film stress between the substrate and the thin film composite electrode due to fabrication and exposure to high-temperature. The technique successfully mitigated the formation of hillocks and material agglomeration as revealed by the SEM images obtained, and can be easily extended to other metallic or composite thin films.**

Keywords—Graded thin film fabrication; high-temperature SAW; composite electrode.

I. Introduction

Surface Acoustic Wave (SAW) devices have been considered for a variety of high-temperature sensor applications, including temperature monitoring, gas sensing, and strain measurement [1], [2]. Commercially available langasite (LGS) crystal cuts have been used for high-temperature SAW sensor applications due to the crystal capability of retaining its crystal integrity and piezoelectric properties at temperatures above 1100°C [2], [3].

Regardless of the application, sensor stability after high-temperature shock, soaking, or cycling is critical for most practical sensor applications. For high-temperature SAW operation both the piezoelectric thin film or crystal and the thin electrode film must be stable, and the stability of the latter is one of the limiting factors for increasing the temperature of operation [2].

Films consisting of Pt-Al_2O_3 and other Pt-alloys composite thin-films have been effectively used as SAW sensor high-temperature electrodes, degrading with time after exposures to temperatures above 800°C, particularly due to material agglomeration and hillock formation [2], [4]-[6]. Both hillock and agglomeration phenomena are assumed to be strongly influenced by stresses in the Pt-Al_2O_3 composite film generated by the deposition process and the difference in expansion coefficients between the LGS substrate and the Pt-Al_2O_3 composite film when the sensor is heated from room temperature to 850°C or above.

In this work a modified multilayer thin-film structure is proposed and implemented, aimed at mitigating hillock formation and material metal agglomeration to improve the Pt-Al_2O_3 composite electrode stability. The technique implemented consists in depositing a metallic buffer layer on top of the Zr adhesion layer, followed by a graded transition from Pt to the Pt-Al_2O_3 composite film. The rationale is that the metallic Pt buffer layer allows the mitigation of agglomeration and hillock formation by better accommodating stresses than the Pt-Al_2O_3 composite film alone. Scanning Electron Microscopy (SEM) images revealed an excellent improvement in the mitigation of hillock formation and material agglomeration after the new multi-layered thin-film electrode structure has been cycled in air above 710°C for over 240 hours and above 840°C for 300 hours.

II. Film Composition and Deposition

In order to verify the performance of the newly proposed Pt-Al_2O_3 electrode structure, it was compared with the previously reported Pt-Al_2O_3 fabrication method [5]-[7]. The film fabricated using the previous method, henceforth **Film 1**, consists of a 10nm thick Zr adhesion layer deposited using e-beam evaporation on the LGS substrate, followed by a composite Pt-Al_2O_3 electrode with a thickness of 170nm, for a total film thickness of 180nm. The composite Pt-Al_2O_3 electrode is fabricated at 82% Pt and 18% Al_2O_3 by co-evaporation of Pt and Al in an oxygen environment at partial pressure of 10^{-5} Torr. The modified Pt-Al_2O_3 electrode structure, henceforth **Film 2**, consists of a 10nm Zr adhesion layer, followed by 10nm of a pure Pt layer, followed by 10nm of a graded transition layer from Pt to the Pt-Al_2O_3 composite electrode, and a final 150nm of the regular Pt-Al_2O_3 composite, for a total film thickness of 180nm.

One port SAW resonators (SAWRs) were fabricated on commercially available LGS Euler angles {0°, 138.5°, Ψ} wafers at the University of Maine Frontier Institute for Research in Sensor Technologies (FIRST) cleanroom facilities using liftoff photolithography and the e-beam evaporation introduced in the previous paragraph. Devices oriented along third Euler angles Ψ = 26.7° and Ψ = 77.7° were fabricated and used in this

This work has been funded by the U.S. Department of Energy/National Energy Technology Laboratory (NETL) under grant number DE-FE0026217

work with the following parameters: 1:1 mark-to-space ratio; nominal operational frequency around 190MHz; 411 reflectors on either side of the interdigitated transducers (IDTs); 161 IDT electrodes for $\Psi = 26.7°$ and 241 IDT electrodes for $\Psi = 77.7°$; acoustic aperture of 51λ for $\Psi = 26.7°$ and 61λ for $\Psi = 77.7°$. Both Ψ orientations 26.7° and 77.7° were fabricated in the same mask, and have power flow angle of 0° and -16°, respectively. In order to deposit the electrodes evenly on the different orientations, the samples were rotated 360° every 22 seconds for the entire duration of the deposition.

III. Experimental Procedure

After fabrication, the wafers were rinsed with acetone, iso-propanol, methanol and de-ionized (DI) water and dried in N_2 flow. At this point, Scanning Electron Microscopy (SEM) images were obtained of the devices containing both Film 1 and Film 2, which will be label henceforth "as fabricated". After that, the wafers were heated in an alumina crucible to 800°C for four hours in air as a means of annealing and activating the Pt-Al_2O_3 electrodes (reducing the electrode resistivity) for SAW operation [5], [6]. The wafers were then cleaned, and SEM images were obtained once again for both types of films. Finally, the wafers were covered with photoresist and diced into 10x3x0.5mm^3 device chips.

Fig. 1 shows the experimental setup utilized for the high-temperature tests reported in this work. The heating was performed using a Thermolyne box furnace 48000. For continuous-time monitoring, devices of each film type were mounted on an Inconel plate secured in place by 4mil Pt wire. The electrical connections between the high-temperature coaxial cable and the SAWRs were made using 1mil Pt wire. A K-type thermocouple (TC) was used on the rear side of the Inconel plate to monitor its surface temperature. The setup was introduced into the furnace as demonstrated in Fig. 1 and interrogated using an NI 9213 module for the TC and an Agilent 8753D Vector Network Analyzer (VNA) for the SAWRs. The temperature was recorded before and after each frequency sweep for both devices (VNA frequency sweep: 10MHz centered at 190MHz with 1601 points and an Intermediate Frequency (IF) bandwidth of 3kHz). The before and after temperature readings were averaged to associate a temperature to the respective sweep. Parabolic fitting over a bandwidth of 25kHz was implemented to determine the resonant frequency value. The temperature and frequency sweep measurements took a few seconds, which were repeated every 30 seconds. Alongside the time-monitored devices, extra SAWRs of both film compositions were placed in an alumina crucible and exposed to the same cycling. SEM images were obtained after cleaning these devices before and after each temperature cycling experiment described in the next paragraph.

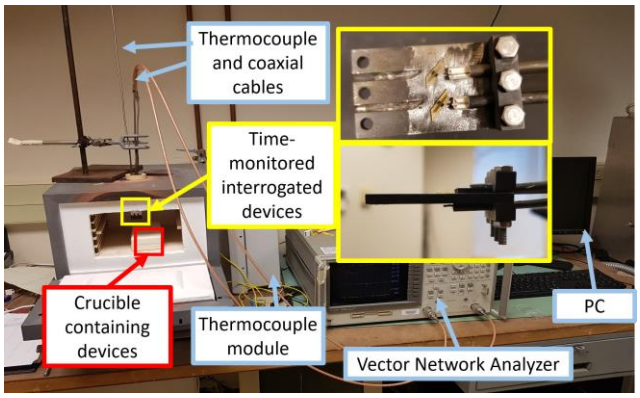

Fig. 1. Experimental setup

Two different temperature cycling profiles were adopted for the tests. Profile 1 consisted of four cycles between 750°C and 300°C (furnace set-up temperatures) with one-hour holding time at each of these values, followed by a soaking period of 10 hours at 750°C, another similar four cycles between 300°C and 750°C, and a final two-hour hold time at 300°C. Profile 2 consisted of the same hold times with a temperature variations between 890°C and 350°C (furnace set-up temperatures) instead of 750°C and 300°C. Fig. 2 shows the actual temperature recorded by the TC mounted at the Inconel plate for both temperature cycling profiles. The period of each profile will be referred henceforth as one round. The temperature plateau values were averaged, and have standard deviation smaller than 1.5°C.

IV. Results and Discussion

Fig. 3 shows the progression of SEM images of SAWRs IDTs for both Film 1 (left column) and Film 2 (right column). The two images in the first row, State 1, depict the devices as fabricated. One should note that the fabricated electrodes are thinner than the nominal value away from the electrode center due to photoresist shadowing during the rotation of the wafer holder for the film deposition described in Section II. Overall, only about 40% of the electrode width has the nominal thickness described in Section II. As can be seen from the Fig. 3, both films are indistinguishable at State 1, with smooth surfaces and no signs of deterioration.

The two SEM images in the second row of Fig. 3, State 2, depict the same IDT region of the SAWRs after exposure to 800°C for four hours (electrode activation, described in Section III). As can be observed from these images, Film 1 (State 2 left) already shows the formation of stress hillocks and material agglomeration, ranging in diameter from 400nm to 1000nm and a density of approximately 1 hillock/3um^2 (0.35 hillocks/μm). The Film 2 graded structure (State 2 right) shows no sign of hillock formation nor any material agglomeration after exposure to the same 800°C for four hours in air.

State 3, the third row in Fig. 3, shows the electrode conditions of both Films 1 and 2 after four repetitions of Profile 1 depicted in Fig. 2, that is four Profile 1 rounds. As can

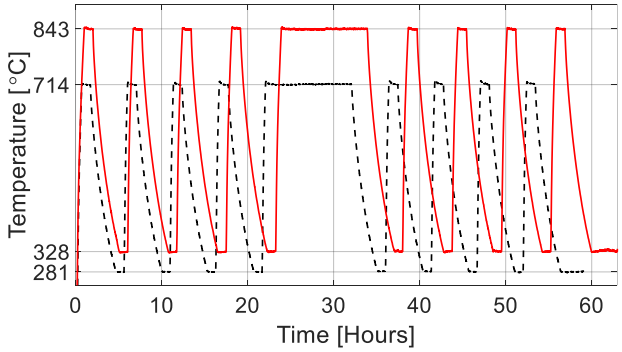

Fig. 2. Temperature readings by the thermocouple mounted on the Inconel plate during one round of the continuous-time monitoring tests for Profile 1 (dashed black line) and Profile 2 (solid red line).

be seen from the images, Film 1 continued to show hillocks ranging from 400nm to 1000nm, whereas Film 2 still showed no sign of hillock formation or material agglomeration.

Finally, State 4, the last row in Fig. 3, shows Film 1 and Film 2 conditions after five consecutive rounds of Profile 2 (Fig. 2). Upon exposure to multiple cycling between 328°C and 843°C, the thinner parts of the electrodes as discussed at the beginning of this section, showed signs of agglomeration for both Films 1 and 2. Interestingly, though, the center part of the graded Film 2 electrodes, i.e., the part that has the nominal film thickness of 180 nm seemed to be unaffected by the Profile 2 five rounds of cycling up to 843°C. Film 1, on the other hand, not only suffered severe agglomeration at the thinner part of the electrodes, but also, and more importantly, showed evidence of absence of material at the center part of the electrode, where the nominal thickness is 180 nm. These holes are due to the popping out of the hillocks shown in Stages 2 and 3, combined with further material agglomeration.

The SEM images in Fig. 3 reveal that the new graded film fabrication procedure proposed and implemented in this work successfully addressed the issues of hillock formation and material agglomeration due to film stresses after fabrication and exposure to high temperatures through cycling and soaking periods.

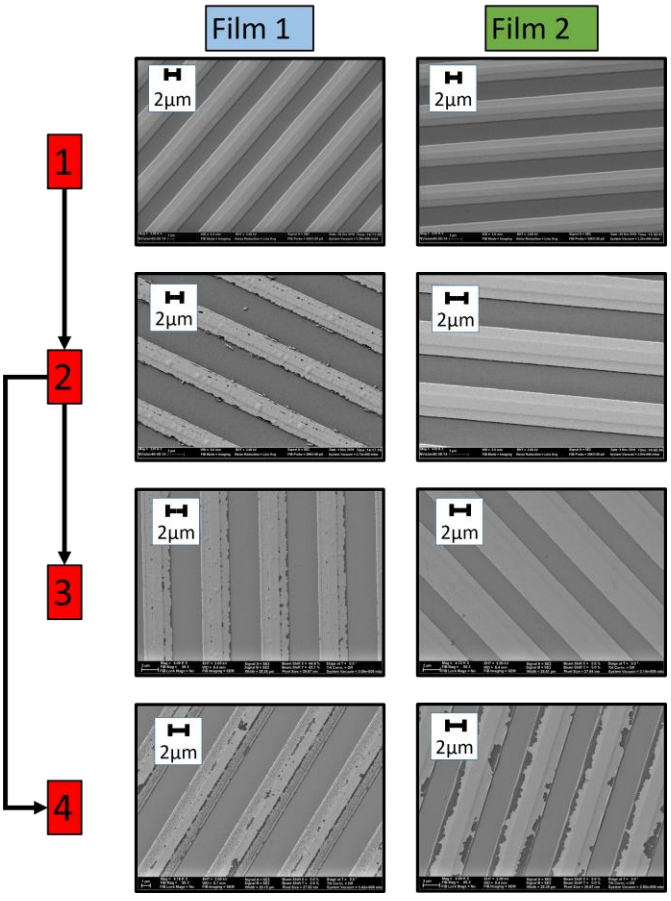

Fig. 3. SEM images for Film 1 (left column) and Film 2 (right column) for the four states discussed in the text. State 1: as fabricated; State 2: 800°C for four hours; State 3: cycled for four rounds of Profile 1; State 4: cycled for five rounds of Profile 2.

Fig. 4 shows SAWRs continuous-time measurements conducted for four rounds of Profile 1. Fig. 4 top shows the four rounds of the Profile 1 temperature cycle (right vertical axis) and the Film 1 SAWR frequency response (left vertical axis) as a function of time. Fig. 4 bottom plots the average frequency variation of the last 30 measurements of each cycling period at the highest temperature, which is shown on the right axis of the plot, for both Film 1 (blue triangles) and Film 2 (green circles) SAWRs, where the reference frequency, f_0, is 188.725MHz for Film 1 and 188.093MHz for Film 2. The two SAWRs whose results are shown in Fig. 4 were fabricated along $\Psi = 26.7°$. The error in the frequency measurements was smaller than 0.002% (comparable or smaller than the size of the shapes used in the figure). One can observe that the resonant frequency variations of the soaking periods are consistently higher than subsequent excursions to the same temperature in the cycles following, revealing that, although the TC mounted on the rear side of the Inconel plate shows a stable temperature, the 1-hour shorter periods are not enough for the device to reach a stable temperature. These differences are less than about 12kHz, which for a temperature sensitivity around 10kHz/°C for this orientation at 700°C corresponds to a maximum temperature difference of 1.2°C. Note that this value of temperature variation is comparable to fluctuations in temperature due to the furnace controller and thermocouple. Therefore, after the middle of the third round one can say that the annealing of Pt-Al_2O_3 electrode for both Films 1 and 2 has been achieved [6] and thus both devices are relatively stable. It is interesting to note that both Film 1 and Film 2 possess similar stabilization responses,

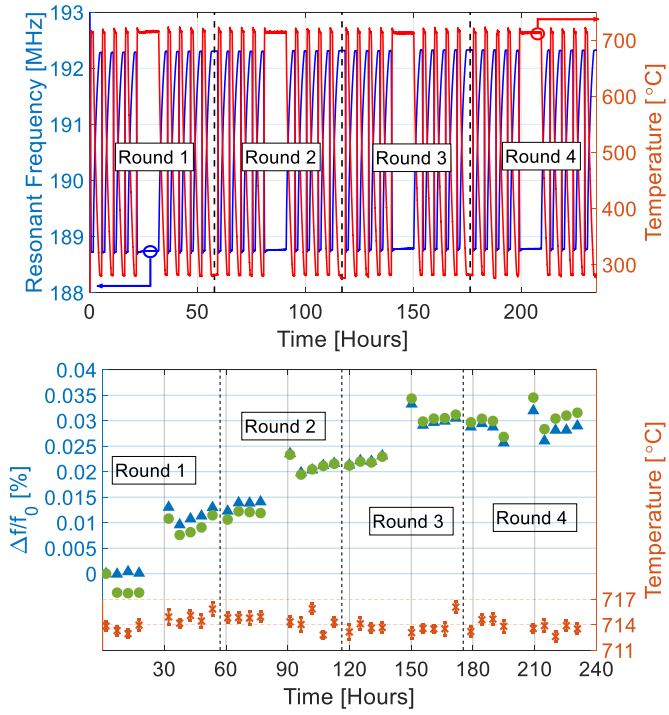

Fig. 4. Continuous-time monitoring frequency measurements for Films 1 and 2. Top plot: Profile 1 temperature cycling and the respective Film 1 frequency response; Bottom plot: averaged relative frequency variation for Film 1 (blue triangles) and Film 2 (green circles) at the maximum temperature value shown on the right axis (f_0, Film 1: 188.725MHz, Film 2: 188.093MHz).

despite the differences in film quality (hillocks and agglomeration) of Film 1 revealed in Fig. 3. This result suggests that stress release and morphologic changes in both Film 1 and Film 2 electrodes are mostly responsible for the electrodes annealing and SAWR stabilization, not only the hillock and agglomeration as originally postulated.

Fig. 5 shows SAWRs continuous-time measurements conducted for five rounds of Profile 2. The figure plots the average frequency variation of the last 30 measurements of each cycling period at the highest temperature shown on the right axis of the plot for both Film 1 (blue triangles) and Film 2 (green circles) SAWRs, where f_0 is 186.539MHz for Film 1 and 186.093MHz for Film 2. The two SAWRs whose results are shown in Fig. 5 were fabricated along $\Psi = 77.7°$. As can be observed from Fig. 5, around 843°C both Films 1 and 2 revealed frequency drifts. The Film 1 SAWR drifted approximately 44kHz after the fourth soaking period (Feature A in Fig. 5), while Film 2 SAWR drifted approximately 113kHz (Feature B). Subsequently Film 1 SAWR drifted approximately 39.4kHz after the fifth soaking period (Feature C), while Film 2 SAWR drifted approximately 85.8kHz (Feature D). These frequency variations can be correlated to the significant electrode variations seen in Fig. 3 Stage 4 for both Films 1 and 2. The continuous-time monitoring frequency experiments for Profiles 1 and 2 should be repeated with devices fabricated with no wafer rotation, thus avoiding the shadowing and the variation of thickness across the IDT width. Under such fabrication conditions, and based on the SEM images of Fig. 3, in particular the center part of the electrode of nominal thickness 180nm, one should expect that the graded Film 2 will lead to SAWR stable responses at temperatures higher than the devices fabricated with Film 1.

V. Conclusion

The thin film grading fabrication technique introduced in this work successfully mitigated the formation of stress hillocks and material agglomeration of Pt-Al_2O_3 based electrodes exposed to cycling temperatures up to 843°C, as revealed by SEM images that compared films fabricated with the proposed technique to films fabricated using the previously reported procedure.

The fabrication of SAWRs oriented along multiple orientations utilized in this work relied on the rotation of the samples during electrode deposition, which resulted in electrode thickness variation along the width of the IDT. Most likely for this reason, the lack of hillock formation and agglomeration observed from the SEM images at the center of the electrodes fabricated using the graded technique could not be reflected in improvement of SAWR stability response at the highest temperatures measured (843°C). New device fabrication and tests without sample rotation are necessary to verify this statement.

The removal of hillocks and material agglomeration due to film stress after fabrication and exposure to high temperatures achieved by the graded Pt-Al_2O_3 thin film fabrication technique can be extended to other composite thin films. The technique has potential to significantly impact thin film stability under exposure to high-temperature soaking and cycling, which reflects in the stability of devices using such thin film electrodes, in particular SAW-based devices.

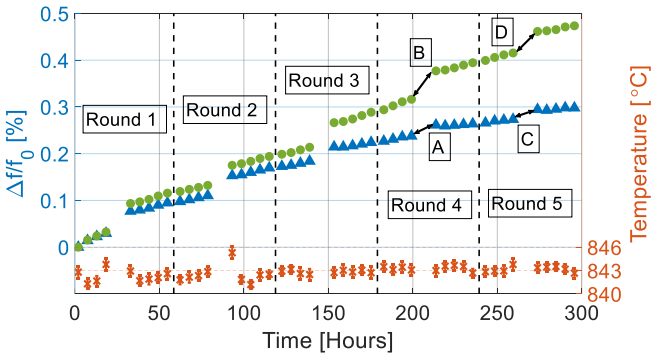

Fig. 5. Continuous-time monitoring frequency measurements for Films 1 and 2 under temperature Profile 2. Averaged relative frequency variation for Film 1 (blue triangles) and Film 2 (green circles) at the maximum temperature value shown on the right axis (f_0, Film 1: 186.539MHz, Film 2: 186.093MHz).

Disclaimer

This work was supported by U.S. Department of Energy Award #: DE-FE0026217. Disclaimer: This report was prepared as an account of work sponsored by an agency of the United States Government. Neither the United States Government nor any agency thereof, nor any of their employees, makes any warranty, express or implied, or assumes any legal liability or responsibility for the accuracy, completeness, or usefulness of any information, apparatus, product, or process disclosed, or represents that its use would not infringe privately owned rights. Reference herein to any specific commercial product, process, or service by trade name, trademark, manufacturer, or otherwise does not necessarily constitute or imply its endorsement, recommendation, or favoring by the United States Government or any agency thereof. The views and opinions of authors expressed herein do not necessarily state or reflect those of the United States Government or any agency thereof.

References

[1] H. Zu, H. Wu, and Q. M. Wang, "High-Temperature Piezoelectric Crystals for Acoustic Wave Sensor Applications," *IEEE Trans. Ultrason. Ferroelectr. Freq. Control*, vol. 63, no. 3, pp. 486–505, Mar. 2016.

[2] M. Pereira da Cunha, "Wireless sensing in hostile environments," *IEEE Int. Ultrason. Symp. IUS*, 2013, pp. 1337–1346.

[3] D. W. Greve, T. L. Chin, P. Zheng, P. Ohodnicki, J. Baltrus, and I. J. Oppenheim, "Surface acoustic wave devices for harsh environment wireless sensing," *Sensors (Switzerland)*, vol. 13, no. 6, pp. 6910–6935, 2013.

[4] M. Pereira da Cunha, R. J. Lad, T. Moonlight, G. Bernhardt, and D. J. Frankel, "High temperature stability of langasite surface acoustic wave devices," in *Proceedings - IEEE Ultrasonics Symposium*, 2008, pp. 205–208.

[5] S. C. Moulzolf, R. Behanan, T. Pollard, R. J. Lad, and M. Pereira da Cunha, "Capacitively coupled IDT for high temperature SAW devices," *IEEE Int. Ultrason. Symp. IUS*, 2013, pp. 255–258.

[6] A. Maskay, A. Ayes, and M. Pereira da Cunha, "Stability of Pt/Al2O3-based electrode langasite SAW sensors with Al2O3 capping layer and yttria-stabilized zirconia sensing layer," *IEEE Int. Ultrason. Symp. IUS*, 2017, pp. 2–5.

[7] D. J. Frankel, S. C. Moulzolf, M. Pereira da Cunha, and R. J. Lad, "Influence of composition and multilayer architecture on electrical conductivity of high temperature Pt-alloy films," *Surf. Coatings Technol.*, vol. 284, pp. 215–221, 2015.